Rev. Adv. Mater. Sci. 31 (2012) 109-115

AGING BEHAVIOR AND PROPERTIES OF ULTRAFINE-GRAINED ALUMINUM ALLOYS OF Al-Mg-Si SYSTEM

E.V. Bobruk, M.Yu. Murashkin, V.U. Kazykhanov and R.Z. Valiev

Institute of Physics of Advanced Materials, Ufa State Aviation Technical University, 12 K. Marx str., Ufa 450000, Russia

Received: April 20, 2012

Abstract. This work is focused on the study of the features of ultrafine-grained (UFG) structure formation, mechanical properties and electrical conductivity of the aluminum alloys of Al-Mg-Si system subjected to severe plastic deformation (SPD). High strength of the material under study is provided by UFG state due to the decrease in grain size and formation of hardening phase precipitations in the aluminum matrix after aging. The increased electrical conductivity in the material results from the decrease in concentration of the alloying elements in the aluminum matrix because of solid solution decomposition during SPD processing and also less dislocation density in the formed structure.

1. INTRODUCTION

It is known that in electrical engineering the application of commercially pure aluminum, the material that possesses the highest electrical conductivity among aluminum materials, is restricted due to its low strength [1-3]. Increase of strength properties of aluminum is achieved by means of inclusion of certain alloying additive elements, such as, for example, magnesium and silicon, i.e. by making the alloys of Al-Mg-Si system [2,3]. Possessing good technological effectiveness and high corrosion resistance, the Al-Mg-Si alloys are widely used as the materials for electrical products; however, the area of their application is considerably limited due to low strength [1,2]. One of the advanced approaches for enhancing properties of aluminum alloys is refinement of their grain structure to ultrafine-grained (UFG) state by such SPD techniques as high pressure torsion (HPT) [4] and equal channel angular pressing with parallel channels (ECAP-PC) [5,6]. Moreover, it is known that the level of properties of the UFG alloys processed by SPD in combination with heat treatment is significantly influenced by changes of the content of alloying elements in solid solution and phase composition. This work deals with the peculiarities of UFG structure formed during SPD and subsequent heat treatment, its connection to mechanical and electrical properties in aluminum heat hardenable alloys of the Al-Mg-Si system. Besides, there is information on phase composition changes in the alloys of this system both in the course of SPD and during subsequent thermal action.

2. EXPERIMENTAL

Commercial AD31 (Russian analogue of the Al alloy 6063) (0.60Mg-0.45Si-0.24Fe-balance Al (wt.%) and 6060 (0.55Mg-0.50Si-0.10Cu-0.10Mn-0.05Cr-0.30Fe-balance Al (wt.%)) alloys were used in a hot-pressed condition. Prior to SPD, initial billets were subjected to solid solution treatment for 2 h at 530 °C with subsequent water quenching. Presently, HPT is a technique that allows the forming of UFG structure with a grain size of 100 nm and less with

Corresponding author: E.V. Bobruk, e-mail: e-bobruk@yandex.ru

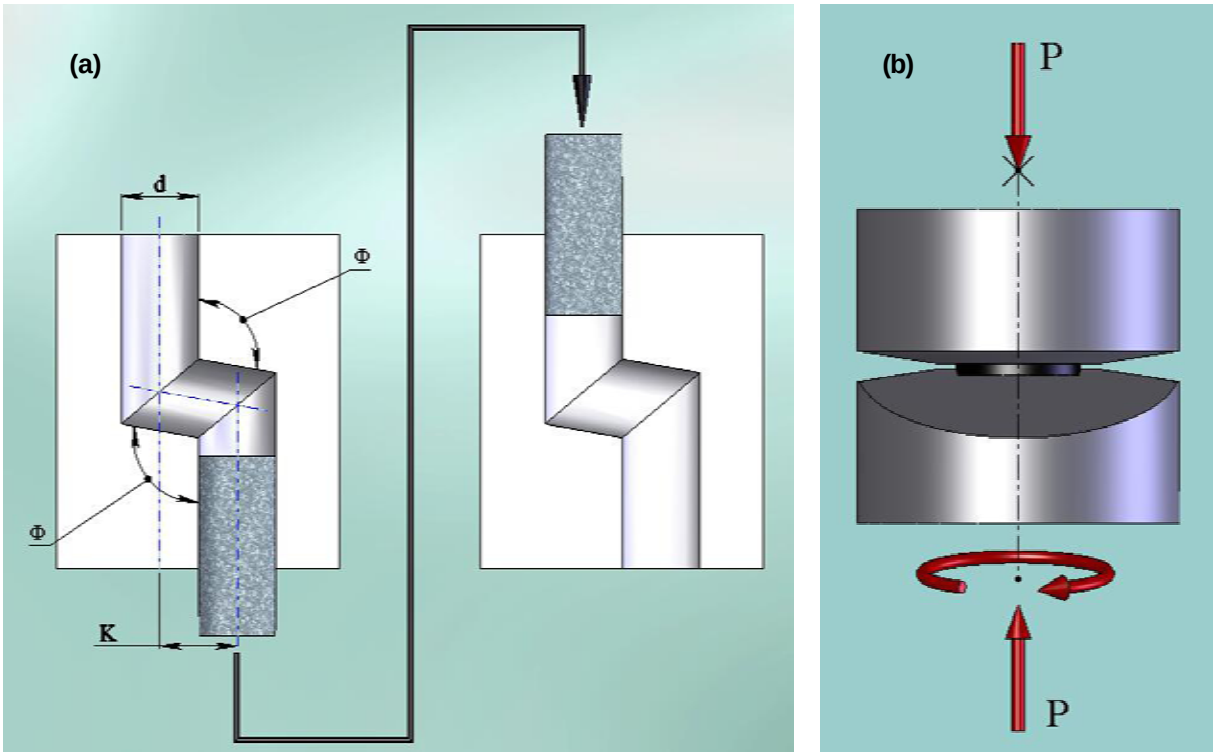

Fig. 1. (a) - The general view of ECAP-PC: a schematic illustration where *d*-diameter of the channel; *K*- is distance axes of the parallel channels; Φ - is the intersection angle of the parallel channels and the channel, which connects them; (b) - The general view of HPT.

high-angle misorientations of boundaries in the aluminum alloys [7,8]. Study of the influence of HPT on the peculiarities of UFG structure and mechanical properties of the low-alloyed Al-Mg-Si alloys is of great interest and has not yet been conducted. Producing of UFG material on a commercial scale calls for manufacturing of equipment that would increase the efficiency of ECAP-processing [6]. To produce long-length billets, the ECAP technique was modified into ECAP-PC [8,9]. The general view of ECAP-PC is shown in Fig. 1a, which distinctive feature is that during a single processing pass, two distinct shearing actions take place: shear in two deformation zones corresponding to two subsequent channels intersections in the die-set (Fig. 1a). Billets of AD31 Al alloy with a diameter of 18 mm and length of 100 mm were subjected to ECAP-PC at 100 °C, since the temperature provides significant grain refinement, preserving the facility for its further strengthening by subsequent aging at 160-175 °C [2].

Billets of 6060 Al alloy with a diameter of 20 mm and thickness of 1.5 mm were subjected to HPT (Fig. 1b) both at room temperature (RT) and at the temperature of 180 °C for the formation of UFG structure. Vickers hardness (HV) was measured using a Micromet-5101 microindentation tester with a load of 0.5 N for 15 s. Each sample was measured more than 10 times to provide reliable results.

Tensile tests at RT were performed on the Instron 1185 machine at a strain rate of 1 mm/min. Mechanical properties were measured on at least 3 specimens with gage length of 15 mm and diameter of 3 mm. Tensile specimens were cut out parallel to the longitudinal axis of the ECAP-processed material. Mechanical tensile tests of flat samples after HPT with gauge part $2.0 \times 1.0 \times 0.8$ mm were performed at RT on a special machine equipped with laser extensometer P50 Fiedler Optoelectronics that provides record of the traverse during tension of a sample with a precision of up to 0.1 μm.

Specific electrical resistivity (r) was determined in accordance with the Russian standard [10] by micro-ohmmeter BSZ. Specific electrical conductivity (ω) of the samples was determined with the help of eddy current device VE-27NS/4-5 for measurement of specific electrical conductivity of nonferrous metals and alloys.

The structural characterization by transmission electron microscopy (TEM) was performed in JEOL-2100 EX electron microscope using dark and bright fields. The average grain size was calculated from more than 250 grains measurement.

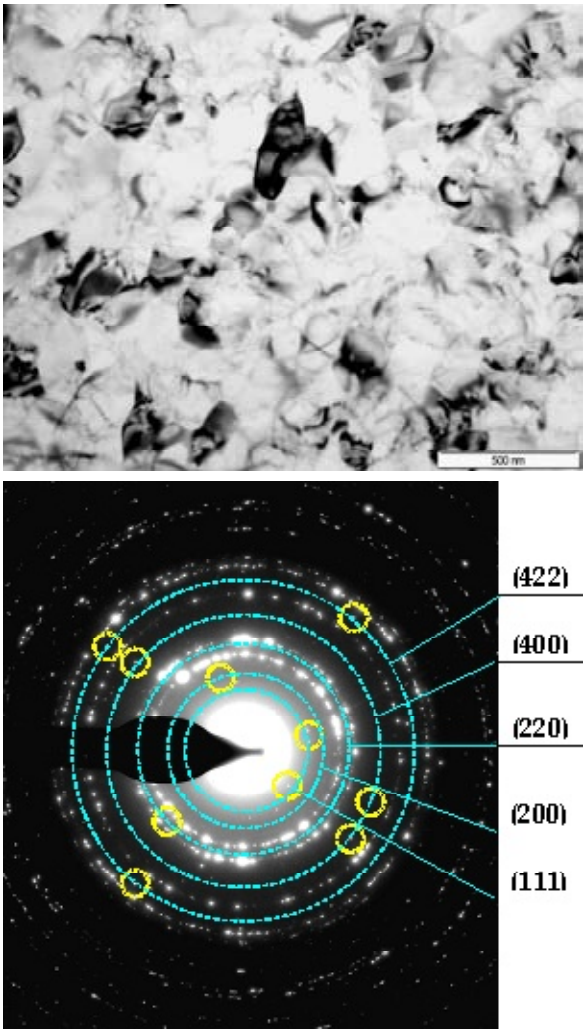

Fig. 2. (a) - UFG structure after HPT at RT; (b) - SAED pattern.

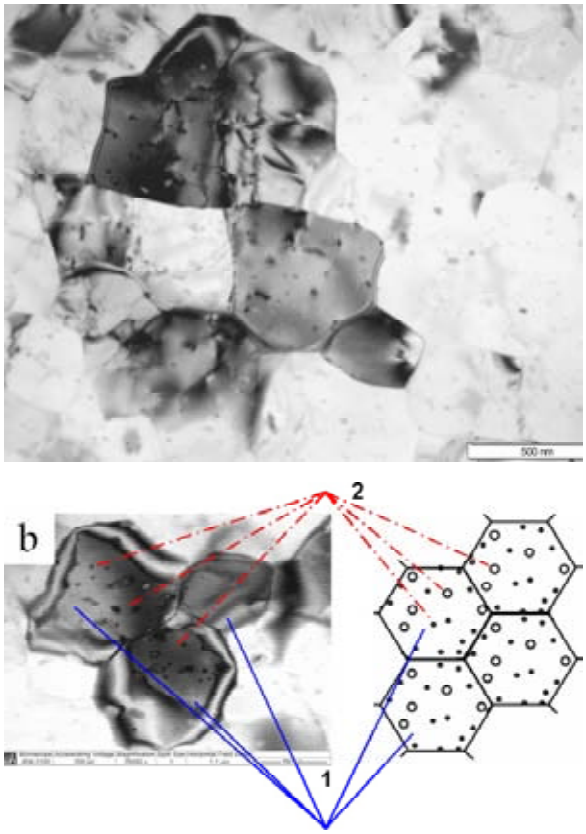

Fig. 3. (a) - UFG structure after HPT at 180°C; (b) - Schematic view of UFG structure (1 – grains; 2 – stable β-phase).

The change of concentration of basic alloying elements in aluminum matrix was studied by X-ray diffraction (XRD) analysis on diffractometer Rigaku IV and 3D atom probe on the «Cameca» company device.

3. RESULTS AND DISCUSSION

3.1. Structure peculiarities, mechanical and electrical properties of the 6060 alloy processed by HPT technique

TEM studies in the 6060 alloy billets after HPT processing at RT revealed the formation of homogeneous UFG structure with the mean grain size of 180 ± 15 nm, the grains having shape close to the equiaxed one (Fig. 2a). Blurring of boundary contrast of the formed grains and presence of extinction contours inside them testify to a high level of inner stresses and crystal lattice distortions in the area near boundaries [7]. Alongside with aluminum matrix spots in electron diffraction patterns there were revealed additional spots (Fig. 2b), indicator test of which showed that they belong to a secondary strengthening β-phase Mg_2Si (Table 1) [11]. Presence of β-phase in the aluminum solid solution testifies to the fact that during HPT the formation of UFG structure was accompanied by dynamic strain aging (DSA) [12] already at RT. However, due to the presence of numerous defects in the crystal structure of aluminum matrix and, probably, high dispersion ability it was not possible to detect the Mg_2Si phase in TEM images.

Deformation temperature was increased to 180 °C to provide more complete aluminum solution decomposition during DSA. After HPT processing at this temperature there are precipitates of nanoscale strengthening Mg_2Si phase in the UFG structure of 6060 alloy with the average grain size of 350 ± 15 nm (Fig. 3). The precipitates, judging by morphological characteristics, and in particular globule shape and size of 20-40 nm, belong to their stable

Table 1. XRD-analysis data.

HKL	Intensity (I)	*d*/*n*, Å	*d*/*n*, Å [8]
111	0.40	3.692 ± 0.002	3.690
200	0.10	3.185 ± 0.002	3.190
220	1.00	2.251 ± 0.001	2.250
311	0.15	1.919 ± 0.002	1.920
400	0.20	1.593 ± 0.002	1.590
422	0.40	1.301 ± 0.001	1.301

modification - β-phase, incoherent aluminum matrix [13,14].

The changes of alloy crystal lattice parameter established by XRD analysis and 3D atom probe data (Table 2) testify that after HPT processing at 180°C the concentration of alloying elements in the UFG matrix decreases by an order of magnitude in the course of DSA, getting close to that of pure aluminum. Thus, UFG condition provides for high alloy strength by means of grain size decrease in accordance with the Hall-Petch relation [15,16] and for generation of strengthening phase dispersive precipitates in the aluminum matrix – precipitation hardening [13]. Ultimate tensile strength is ~ 40% higher than that after conventional treatment T6 (Table 3). The enhanced electrical conductivity of the material (Table 3) in accordance with [2,17] is provided by less dislocation density in the formed structure and decrease of alloying elements concentration in the aluminum matrix due to decomposition of solid solution in the course of SPD processing. The values of specific electrical conductivity are getting close to those of pure aluminum (Table 3).

3.2. Structure peculiarities, mechanical and electrical properties of AD31 alloy after processing by ECAP-PC technique

Below are the peculiarities of UFG structure formation and regularities of increase in mechanical and electrical properties in the aluminum alloy AD31 of Al-Mg-Si system, processed by 4 passes of ECAP-PC at 100 °C, similar to [18].

TEM studies demonstrated that after ECAP-PC processing in the alloy AD31 UFG structure with the mean grain size of 500 ± 25 nm was formed. Analysis of electron-diffraction patterns testify that UFG structure with predominantly high-angle grain-

Table 2. Microstructural characteristics of aluminum alloy 6060.

Material	Treatment / Structure condition	Lattice parameter, Å	Content of basic alloying elements in the matrix, at. %	Lattice microdeformation, %
6060	Quenching / CG	4.0511 ± 0.0001	0.621Mg 0.861Si 0.017Cu **98.501Al**	0.010 ± 0.009
	T6 / CG	4.0509 ± 0.0001	-	-
	HPT at RT / UFG	4.0506 ± 0.0001	0.400Mg 0.427Si 0.011Cu **99.119 Al**	0.170 ± 0.030
	HPT at 180°C / UFG	4.0498 ± 0.0001	0.052Mg 0.088Si 0.006Cu **99.837Al**	0.030 ± 0.010
CP Al	Annealing / CG	4.0495 ± 0.0001	99.6	-

Table 3. Mechanical and electrical properties of aluminum alloy 6060.

Material	Treatment / Structure condition	UTS,MPa	El.,%	$\omega_{20°C}$,MS/m	IACS,%
6060	Quenching / CG	187 ± 3	20 ± 0.5	30.3	52.0
	T6 / CG	250 ± 2	8 ± 0.4	31.1	53.6
	HPT at RT / UFG	525 ± 2	5 ± 0.4	29.4	51.8
	HPT at 180 °C / UFG	347 ± 3	7 ± 0.3	33.7	58.1
CP Al	Annealing / CG	95 ± 1	35 ± 0.5	37.6	62.0

Table 4. Mechanical and electrical properties of aluminum alloy AD31.

Treatment	HV,MPa	YS,MPa	UTS,MPa	El.,%	$\rho_{20°C}$,Ohm*mm²/m	IACS,%
Quenching	450.8 ± 12	50 ± 3	100 ± 2	25.0 ± 0.4	0.03262	52.9
T6	676.2 ± 17	170 ± 3	200 ± 2	14.2 ± 0.3	0.03162	54.5
ECAP-PC at 100 °C	872.2 ± 16	256 ± 2	264 ± 2	13.0 ± 0.3	0.03327	51.8
ECAP-PC + AA	1050 ± 19	289 ± 2	308 ± 1	15.5 ± 0.5	0.02941	58.6

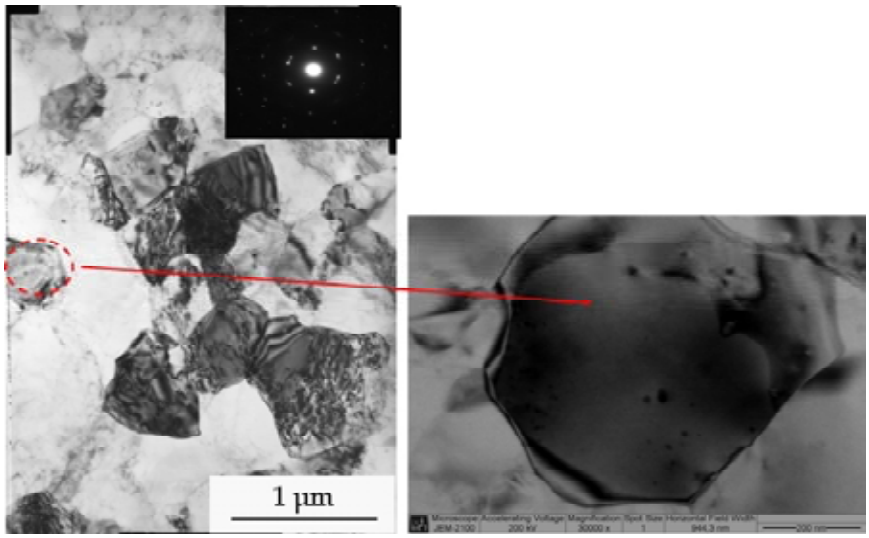

Fig. 4. - UFG structure after ECAP-PC at 100 °C.

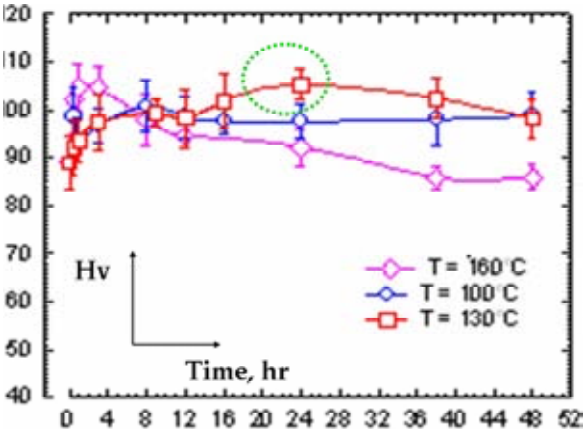

Fig. 5. - Influence of artificial aging on hardness of UFG alloy AD31.

boundary misorientations was formed in the alloy [6,7]. There were also revealed the globule dispersive precipitates of stable strengthening β phase about 10 nm in size, both in the area near boundaries and inside the grains (Fig. 4). Presence of precipitates of this phase testifies that during ECAP-PC the formation of UFG structure in the alloy was accompanied by DSA process. The UFG structure formation in the alloy of Al-Mg-Si system during ECAP-PC, consisting in transformation of elongated subgrains into equiaxed grains by means of their fragmentation, was earlier noted in work [18] devoted to the studies of structure evolution of aluminum alloys during processing by conventional ECAP [6].

Results of mechanical tests of the AD31 alloy samples after ECAP-PC are presented in Table 4. The processed billets demonstrate higher values of hardness, yield stress (YS) and ultimate tensile strength (UTS) than those after conventional treatment T6 to the maximum strength (Table 4).

In order to reveal the possibility of further strengthening of UFG alloy, a part of billets after SPD was subjected to artificial aging (AA), performed within the temperature range of 100…160 °C with holding time of up to 48 hours. After ECAP-PC the AD31 alloy billets demonstrate enhancement of strength with maximums of strengthening after AA performed at 130 °C (Fig. 5). The obtained results testify that after ECAP-PC processing the UFG alloy preserve potential for additional strengthening by means of precipitation hardening.

Investigation of fine structure of the UFG alloy billets strengthened as a result of AA made it pos-

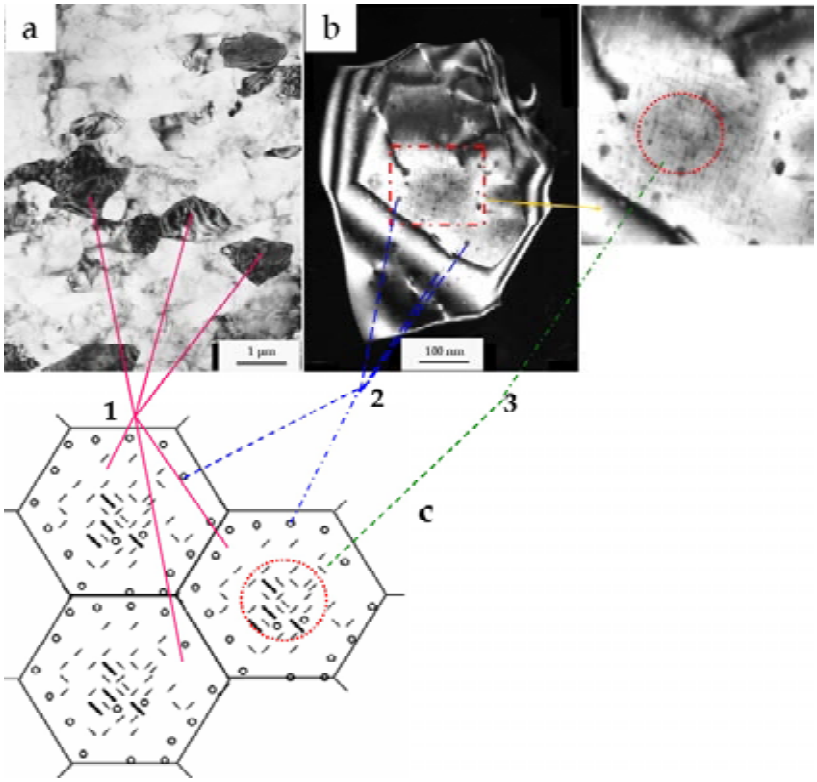

Fig. 6. (a, b) - UFG structure after ECAP-PC at 100°C and subsequent artificial aging; (c) - Schematic view of UFG structure (1 - grains; 2 - stable β-phase; 3 - metastable β' and β"-phase).

sible to establish the cause of strengthening. After AA, alongside with dispersive particles of b-phase, precipitated in the course of SPD, in UFG grains with a size of > 300 nm there was observed generation of nanoscale strengthening particles of β'' and β' phases (Fig. 6). It is known that precipitation of these metastable phases in the aluminum matrix of coarse-grained alloys of the Al-Mg-Si system provides for their strengthening after AA, realized during conventional treatment [13,19-21]. It was also noted that in the grains of less than 300 nm size both after SPD and after additional AA there are only globule precipitates of stable β-phase (Fig. 6). Fig. 6 schematically represents the stages of strengthening of Mg_2Si phase precipitation after ECAP-PC and after additional AA. Thus, it was established that the formation of metastable phases in UFG alloy after AA leads to additional increase in its strength (Table 4).

The established peculiarities of structure and hardness changes in the UFG alloy billets after SPD and subsequent AA well coincide with the mechanical test results. Maximum strength was achieved in the AD31 alloy billets after ECAP-PC and subsequent aging by selected regime, UTS of the alloy increased by 54% in comparison with conventionally strengthened condition (T6) (Table 4). The YS value of the alloy after processing by the abovementioned regimes increased to a more considerable value by 76% and El. made 15% (Table 4).

Thus, it was demonstrated that the defined precipitation of strengthening particles of β", β' and β phases in the ultrafine grains, realized both on the stage of SPD processing and during subsequent AA, provides a considerable increment of strength properties preserving ductility.

Taking into account that grain boundaries (with a size of grains over 400 nm) and nanoscale particles of strengthening phases at room temperature are not a significant barrier on the way of conductivity electron motion, and the matrix with lower concentration of alloying components provides increase of specific electrical conductivity value (ρ), it can be stated that the formation of UFG structure in the aluminum alloys Al-Mg-Si by ECAP-PC and AA in the selected regime creates the conditions for achievement of not only high strength, but also high electrical conductivity in the alloy. In UFG condition the AD31 alloy demonstrates UTS = 308 MPa, ρ = 0.02941 Ohm*mm^2/m and 58.6% IACS (International Annealed Copper Standard), and in condition

after conventional strengthening treatment UTS = 200 MPa, ρ = 0.03162 Ohm*mm^2/m and 54.5% IACS, correspondingly (Table 4).

4. CONCLUSIONS

It is demonstrated that both SPD techniques can be successfully utilized for grain refinement down to the ultra-fine scale in the Al-Mg-Si alloys. The ultra-fine grained Al-Mg-Si alloys containing second phase nano-precipitates show increased strength and enhanced electrical conductivity:

The increased strength is due (1) to the grain size strengthening according to the well known Hall-Petch law, (2) to the presence of stable and metastable second-phase nanoprecipitates providing precipitation hardening, and (3) to the strain hardening mechanism.

The increased electrical conductivity of the UFG material can be rationalized in terms of the formation of the second-phase precipitates which absorb the main alloying elements (Mg and Si), thus, decreasing their concentration in the Al matrix.

ACKNOWLEDGEMENTS

Authors are grateful to Dr. G.I. Raab for SPD processing.

REFERENCES

[1] I.B. Peshkov // *Cables and wires* **1** (2009) 314.
[2] L.A.Vorontsova, V.V. Maslov and I.B. Peshkov, *Aluminum and aluminum alloy in electrical products* (Energies, Moscow, 1971, p. 224)
[3] S. Koch, *BHM* **152** (2007) 62.
[4] A.P. Zhilyaev and T.G. Langdon // *Prog. Mater. Sci. V* **53** (2008) 893.
[5] G.I. Raab // *Mater. Sci. Eng. A* **410-411** (2005) 230.
[6] R.Z. Valiev and T.G. Langdon // *Prog. Mater. Sci. V* **51** (2006) 881.
[7] R. Z. Valiev, R. K. Islamgaliev and I. V. Alexandrov // *Progr. Mater. Sci. V* **45** (2000) 103.
[8] Y. Estrin, M. Murashkin and R. Valiev, In: *Fundamentals of aluminium metallurgy: Production, processing and applications*, ed. by R. Lumley (Woodhead Publishing Limited, Cambridge, 2010), p. 468.
[9] G.I. Raab // *Mater. Sci. Eng. A* **410-411** (2005) 230.
[10] Russian standards 7229-76 Cables, wires and cords. Method of measurement of electrical resistance of conductors.
[11] Ya.S. Umanskiy, Yu.S. Skakov, A.N. Ivanov and L.N. Rastorguev, *Crystallography, X-ray diffraction and elecron microscopy* (Metallurgy, Moscow, 1982)
[12] J.K. Kim, H.G. Jeong, S.I. Hong, Y.S. Kim and W.J. Kim // *Scripta Mater. V* **45** (2001) 901.
[13] L.F. Mondolfo, *Aluminum Alloys: Structure and Properties* (Butterworth's, London, 1979), p. 640.
[14] M. Murayama and K. Hono // *Acta Mater. V* **47(5)** (1999) 1537.
[15] E.O. Hall // *Proc. Phys. Soc. London. V* **64B(381)** (1951) 747.
[16] N.J. Petch // *J. Iron Steel Inst. V* **174(1)**. (1953) 25.
[17] Champion, Y. Bréchet // *Adv. Eng. Mater.* (2010) 12: doi: 10.1002/adem.200900346. 798
[18] R. Valiev, M. Murashkin, E. Bobruk and G. Raab // *Mat. Trans. V* **50(1)** (2009) 87.
[19] S.J. Andersen, H.W. Zandbergen, J. Jansen and C. Traeholt // *Acta Materialia.* **46(9)** (1998) 3283.
[20] K. Matsuda, Susumu Ikeno, Tatsuo Sato and Akihiko Kamio // *Mater. Sci. Forum. V* **217-222** (1996) 707.
[21] Yassar Reza S., David P. Field and Hasso Weiland // *Scripta Mater.* **53** (2005) 299.